Morphometric analysis of relic landslides using detailed landslide distribution maps: Implications for forecasting travel distance of future landslides

Tsuyoshi Hattanji*[a], Hiromu Moriwaki[b]

[a] *Graduate School of Life and Environmental Sciences, University of Tsukuba, 305–8572, Japan*

[b] *National Research Institute for Earth Science and Disaster Prevention (NIED), 305–0006, Japan*

* Corresponding author. Tel: +81 29 853 5687; fax: +81 29 853 6879

E-mail address: hattan@geoenv.tsukuba.ac.jp (T. Hattanji)

Abstract

This study analyzed the morphometry of relic landslides in four mountainous areas in Japan. Using detailed landslide maps issued by the National Research Institute for Earth Science and Disaster Prevention of Japan, the mobility of 338 relic landslides was evaluated based on the *H*/*L* ratio, i.e., the equivalent coefficient of friction. The *H*/*L* ratio strongly correlates with the initial slope, tanθ_r (R^2 = 0.78–0.88). The *H/L* ratio and tanθ_r of recent disaster-causing landslides within the past few decades were also measured in each investigated area. The data of recent landslides correspond to the 95% lower prediction limit of the tanθ_r–*H*/*L* regression line for relic landslides. This result implies that morphometric analysis of relic landslides around an unstable mass allows for forecasting of travel distance of the unstable mass.

Keywords: Landslide map, Morphometric analysis, Mobility, Travel distance, Equivalent coefficient of friction

1. Introduction

Landsliding is a major geomorphic process affecting landscape evolution in mountainous regions (Roering et al., 2005), and causing catastrophic disasters. Since natural and human impacts may reactivate some relic landslides (Ost et al., 2003; Chigira and Yagi, 2006), a landslide map based on aerial photographic interpretation is useful for understanding the possibility of landslide reactivation in the future. Analysis of landslide susceptibility using a landslide map has been developed with a multivariate statistical approach (Carrara et al., 1991, 2003; Ayalew and Yamagishi, 2005) and the analytic hierarchy process method (Yoshimatsu and Abe, 2006). However, not only assessment of landslide susceptibility, but prediction of mobility is necessary for mitigation of landslides.

Scheidegger (1973) and Hsü (1975) suggested an index of landslide mobility, *H/L*, where *H* is the fall height and *L* is the horizontal length of an entire landslide. The *H/L* ratio, which is equivalent to the gradient of the line from toe to top of a landslide, is refereed to as the 'equivalent coefficient of friction' from the standpoint of kinematics. Scheidegger (1973) and Hsü (1975) also indicated that the *H/L* ratio of a rock avalanche decreases with increasing volume of the avalanching mass. Corominas (1996) confirmed this size effect on the *H/L* ratio for other types of landslides. Moriwaki (1987) revealed that the *H/L* ratio decreases with decreasing initial slope for both natural and experimental landslides. Recent statistical analyses for shallow landsliding also ensured the effects of topography on the *H/L* ratio (Finlay et al., 1999; Hunter and Fell, 2003; Okura et al., 2003).

The above studies used various datasets of recent landslides, which may include landslides under diverse local environmental conditions such as geologic, topographic and climatic. Nevertheless, a landslide map provides *H/L* ratios and related parameters for the target area. Few studies, however, quantitatively measured landslide mobility based on a large data set from landslide maps.

Moriwaki and Hattanji (2002) obtained the mobility of relic landslides in three landslide-prone areas by using detailed landslide maps issued by the National Research Institute for Earth Science and Disaster Prevention of Japan (NIED). The NIED landslide maps are based on the interpretation of 1:40 000 aerial photographs, and distinctly show crowns, flanks, and displaced masses of moderate-scale relic landslides (>100 m in width) on 1:50 000 topographic maps (Fig. 1). Moriwaki and Hattanji (2002) reported that the *H/L* ratio strongly correlates with the initial slope of the relic landslides, and they hypothesized that morphometric analysis of relic landslides is useful for forecasting the travel distance of future landslides under similar environmental conditions.

A problem remaining to be solved is the practicability of morphometric analysis to forecasting. For the analysis of relic landslides, subsequent erosion may alter the topography and affect the regression line of initial slope and *H/L* ratio accordingly. To make the morphometric analysis more practical for forecasting, it is essential to compare the outputs from the analysis of relic landslides with those of recent disaster-causing landslides. In addition, this previous study only focused on major landslide-prone areas where the landslide-area ratio is extremely high (20 – 30%). Recent disaster-causing landslides, however, have occurred in areas with relatively low landslide-area ratios (< 10%) as well as in major landslide-prone areas. It is necessary to apply the morphometric analysis for more diverse geomorphic conditions.

(Fig. 1)

We analyze the morphometry of relic landslides in four mountainous areas in Japan where landslide disasters have occurred within the past few decades (Fig. 2). Then we compare results of the morphometric analysis of these relic landslides with those of recent landslides in the same region. Finally, we discuss application of this analysis using landslide maps to forecast the travel distance of future landslides.

(Fig. 2)

2. Investigated areas and recent landslide disasters

2.1. *Description of the investigated areas*

Table 1 shows the geologic, climatic, and geomorphic conditions of four investigated areas: Hachimantai, Nagano, Gojo, and Ichinomiya. Each area covers 706.9 km^2, which is equivalent to a circle with a radius of 15 km. The climate of all the areas is classified as humid temperate, though temperature and precipitation conditions vary regionally. Snow accumulates over 2 m for the Hachimantai area, and less than 1 m for the other areas. Planted and natural forests are the dominant vegetation in most of these areas.

Hachimantai is an active volcanic area where geothermal activities around the volcanoes stimulate landsliding. Structures of several old calderas also control the distribution of large-scale landslides (Oyagi and Ikeda, 1998). These factors are the cause of the high percentage of landslide area (23.1%). The Nagano area consists of both uplifted mountains underlain by Neogene rocks and an inactive Quaternary volcano. The percentage of landslide area increases up to 17.5% for the area excluding a large floodplain of the Shinano River. The Gojo and Ichinomiya areas are uplifted mountains underlain by various lithologies. Although both areas have relatively low percentages of landslide area (3 – 6%), landslide disaster occurred in each area during the past few decades.

(Table 1)

2.2. Descriptions of recent landslides

2.2.1. Sumikawa landslide – Hachimantai area

A landslide occurred at a headwater of the Akagawa River in the Hachimantai area on May 11, 1997 (Fig. 3a). The displaced mass was composed of Quaternary volcanics, including tuff and breccia. This site was previously identified as a relic landslide on the landslide map ‘Hachimantai’ published in 1984 (Inokuchi, 1998). Matsuura et al. (1998) revealed that groundwater recharge by snowmelt and heavy rainfall (110 mm) on May 8 triggered the 1997 landslide. Steam explosions (the star symbol in Fig. 3a) followed immediately after the landslide, and the displaced mass converted to a series of debris avalanches that traveled 2 km downstream along the Akagawa River (Chigira et al., 1998; Hayashi et al., 1998).

(Fig. 3)

2.2.2. Jizukiyama landslide – Nagano area

The Jizukiyama landslide occurred in a suburb of Nagano City in 1985. The underlying geology is weathered Neogene rhyolite tuff. The Nagano Prefectural Government office found small extension cracks on the slope in 1981, and installed extensometers in May 1984. The creep rate was gradual in June 1985 but rapidly accelerated after a thunderstorm that produced 58 mm of rainfall on July 20. The unstable mass slid at 5:00 pm on July 26, and flowed into residential areas (Fig. 3b). A southward flow involving a welfare facility caused 26 deaths, and two eastward flows buried about 50 houses (Oyagi et al., 1986).

2.2.3. Wada landslide – Gojo area

The Wada landslide occurred at a valley-side slope of the Niu River in the Gojo area on August 4, 1982 (Fig. 3c). The underlying geology is Mesozoic slate of the

Chichibu zone. The landslide was located at a section of a relic landslide (Okunishi and Okuda, 1982). After heavy rainfall of 350 mm from August 1 to 3, a local resident observed a small crack on the slope. The crack rapidly extended and two landslides occurred at 2:00 and 8:15 am on August 4. The displaced mass temporally dammed up the Niu River, causing flooding in a major residential area on the opposite side of the river (Yonetani et al., 1983).

2.2.4. Fukuchi landslide – Ichinomiya area

The Fukuchi landslide occurred in the Ichinomiya area on September 13, 1976 (Fig. 3d). The landslide was located on a NW–SE fault zone, which borders sedimentary rocks, volcanic rocks, and granodiorite. According to a tradition told in Ichinomiya Town, a large-scale landslide occurred at the same place about 300 years ago (Okunishi, 1982). From September 8 to 12, a typhoon brought 717 mm of rainfall. The large-scale landslide occurred at 9:20 am on September 13, following a small landslide at 6:30 am. The displaced mass transformed into an earth flow, which buried a primary school and many houses. A local resident recorded the landslide process from 9:05 to 9:30 in a sequence of photographs. Although most inhabitants evacuated immediately before the large-scale landslide, three people were reported missing due to the small landslide at 6:30 am (Oyagi et al., 1977; Okunishi, 1982).

3. Morphometric analysis of relic and recent landslides

We used 1:50 000 landslide maps issued by NIED (Shimizu and Oyagi, 1985; Shimizu et al., 1984, 2003, 2004, 2005a,b) for morphometric analysis. To precisely analyze landslide mobility, we selected relic landslides from NIED landslide maps under the following conditions: (a) distinct main scarps, flanks, and outlines of ruptured surfaces, (b) linear movement, and (c) area of ruptured surface greater than 0.01 km^2.

To compare the mobility of the relic and recent landslides, it is necessary to select relic landslides with environmental conditions similar to those of the recent landslides. A simple method is to select relic landslides using the distance from recent landslides *D*. Fig. 4 shows the relationship between *D* and the number of available relic landslides or relative height in the investigated area. The topography of the investigated areas becomes more diverse with increasing *D* as indicated by the increase in relative height. In the case of the Gojo area, the investigated area for D = 20 km includes high-relief mountains (~ 1700 m a.s.l.), while the recent landslide occurred in a low-relief hillslope (~ 400 m a.s.l.). In the Hachimantai and Ichinomiya areas, the numbers of available relic landslide are very small for $D < 10$ km. Consequently, we used relic landslides with $D \leq 15$ km. The number of the landslides is 73 for Hachimantai, 92 for Nagano, 93 for Gojo, and 80 for Ichinomiya.

(Fig. 4)

We followed the methodology of topographic measurement used in our previous research (Moriwaki and Hattanji, 2002). The items measured were the horizontal length and fall height of the entire landslide (L and H) as well as the horizontal length, height, and area of ruptured surface (L_r, H_r, and A_r) (Fig. 5a). The terminology of the measured items is based on the IAEG Commission on Landslides (1990). Although landslide length is often defined by the length along a slope (Cruden and Varnes, 1996), we used horizontal length for convenience. Measuring L_r and H_r is difficult because the outline of the ruptured surface around the landslide foot is generally covered with displaced mass (Fig. 5a). We estimated the outline of the foot from the extrapolation of the outline of the main scarp and flanks, and considered elevation of the lowest ground surface along the extrapolated outline as the elevation of the foot (Fig. 5b).

(Fig. 5)

We measured the morphometry of recent landslides with the same method (Table 2). The L and H measurements for the Sumikawa landslide include those of the debris avalanche (the grey line in Fig. 3a), and L and H of the other landslides were measured along their cross sections, as shown in Figs. 3b-d (i.e., B-B', C-C' and D-D'). We inferred the toe of the ruptured surface from the initial topography and the slip surface in the cross sections. Yonetani et al. (1983) reported that the displaced mass of the Wada landslide reached the opposite bank of the Niu River (toe 2 in Fig. 3c). The cross section steepened at toe 1 (Okunishi and Okuda, 1982, Fig. 3c), which implies erosion of the displaced mass by fluvial processes after the landsliding.

(Table 2)

4. Results and Discussion

4.1 *Effects of landslide size on H/L*

Travel distance is essential for forecasting the area affected by landslides. As noted before, Scheidegger (1973) and Hsü (1975) proposed that the H/L ratio decreases with increasing volume of rock avalanche. However, volume data is not available on the landslide map we used. Many studies show a clear power-law relationship between volume and area of landslides (Innes, 1983; Guthrie and Evans, 2004), implying a positive correlation between depth and volume. We assumed this correlation and used the area of ruptured surface, A_r, as an indicator of size. Fig. 6 shows the H/L ratio plotted against $\log A_r$. A simple least-squared regression yielded low coefficients of determination for all areas (0.08–0.26); however, they are statistically significant ($p < 0.01$).

(Fig. 6)

Most of the relic landslides we analyzed had an A_r range of 0.01 to 1 km^2, which is narrower than that of some previous studies (Scheidegger, 1973; Hsü, 1975; Corominas, 1996). In addition, the effect of the landslide area on *H/L* is less straightforward than that of volume inferred in the previous studies. Even if the volume of landslides was used, Okura et al. (2003) reported no correlation between the volume and *H/L* for shallow landslides under a limited scale (10^3–10^4 m^3). In general, the size effect becomes less obvious under a limited range of size. Hsü (1975) indicated that the *H/L* ratio decreases when the volume exceeds 5×10^6 m^3. This threshold is equivalent to A_r = 0.5 km^2 for an average depth of 10 m, and would be a reason for the stronger correlation in Hachimantai with larger landslides (Fig. 6). Only 2% of all the relic landslides exceeds the threshold of A_r = 0.5 km^2. Therefore, we ignored the size effect for forecasting travel distance in the investigated areas. However, the size effect may be a key factor if a target unstable mass has a larger size than those of this study.

4.2 *Effects of initial slope on H/L*

Moriwaki (1987) and Okura et al. (2003) revealed a correlation between the equivalent coefficient of friction and the initial slope of a landslide, i.e. slope of the ruptured surface, $\tan\theta_r$ (= H_r/L_r, Fig. 5a). Considering the kinematics of a landslide, this correlation means that a gentler slope has a lower residual strength, which determines the gradient of the displaced mass after landsliding. Fig. 7 indicates definite positive correlations of *H/L* with $\tan\theta_r$ for the relic landslides in the four areas. This result is probably associated with long-term landscape evolution, although this is a topic for future studies. Linear least-squares regression analysis gave the following equation for each area:

Hachimantai: $H/L = 0.77 \tan\theta_r + 0.040$ (1a)

Nagano: $H/L = 0.82 \tan\theta_r + 0.034$ (1b)

Gojo: $H/L = 0.91 \tan\theta_r + 0.035$ (1c)

Ichinomiya: $H/L = 0.83 \tan\theta_r + 0.055$ (1d)

(Fig. 7)

These regression lines have much higher coefficients of determination (0.78–0.88) than those of H/L on A_r (0.08–0.26). All the intercepts of Eq. (1) are significantly different from null ($p < 0.05$). The slope of the regression line, however, indicates average reduction of slopes before and after landsliding because the intercepts are relatively small (0.03–0.05). In other words, a smaller slope of the regression line (Eq. 1) means higher mobility of landslides. Landslide mobility of Hachimantai is definitely higher than that of Gojo. A Student's t-test for the difference in the slopes of these regression lines showed that the difference is statistically significant ($p < 0.05$).

The recent landslides were plotted below the regression lines of Eq. (1) for all the four areas (squares in Fig. 7), meaning that the recent landslides had higher mobility compared to the average of the relic landslides. This may reflect the type of landslides. For example, the recent landslides in Hachimantai and Ichinomiya are flow-type landslides (Fig. 3a,d), although the relic landslides in these areas include some other types with lower mobility.

Another possible explanation of the difference between the recent and relic landslides is erosion of the displaced mass after landsliding. For example, the toe of the Wada landslide was eroded by flow of the Niu River after landsliding (Fig. 3c, Yonetani et al., 1983). Although the downslope motion of a landslide leads to a smaller H/L ratio than initial slope, $\tan\theta_r$, several relic landslides in all the areas have H/L ratios greater than $\tan\theta_r$. Although errors of measurement or mapping might have caused this problem, erosion after landsliding also increases the *H/L* ratio. Topographic change by erosion after landsliding is probable in two cases: (1) the displaced mass moves into a river or a high-order stream, and (2) age of landslide initiation is old enough, to allow valley incision or headward erosion that affects topography of the displaced mass. Therefore, lower prediction limits of the regression lines for the relic landslides are more practical for understanding the behavior of future landslides.

Accordingly, we calculated the 95% lower prediction limits for the regression lines of Eq. (1). Since the statistical uncertainty in the slopes of Eq. (1) was negligible for a $\tan\theta_r$ of 0.1 to 0.8, the 95% limits were approximated to the following linear equations (the thick solid lines in Fig. 7):

Hachimantai: $H/L = 0.77 \tan\theta_r - 0.047$ (2a)
Nagano: $H/L = 0.82 \tan\theta_r - 0.040$ (2b)
Gojo: $H/L = 0.91 \tan\theta_r - 0.049$ (2c)
Ichinomiya: $H/L = 0.83 \tan\theta_r - 0.037$ (2d)

The *H/L* ratios of the recent landslides agree well with Eq. (2) for the Hachimantai and Ichinomiya areas, and are only slightly larger than those from Eq. (2) for the other two areas (Fig. 7). Although the number of examples is limited, this result indicates that morphometric analysis of relic landslides is useful for forecasting the travel distance of future landslides under similar environmental conditions.

Regression analysis between $\tan\theta_r$ and the *H/L* ratio for relic landslides enables us to forecast a possible *H/L* ratio of an unstable mass. Requirements for this prediction are the average slope of an unstable mass expected to slide and a detailed landslide map, which separately outlines crowns, flanks, and displaced masses. Table 3 shows the 95% lower prediction limits of the regression lines for D = 5, 10, and 15 km. For the Nagano area where landslide density is higher than that of the other areas, the 95% lower prediction limit even for D = 5 km agrees well with the H/L of the recent landslides. For the Hachimantai and Ichinomiya areas, however, the regression analysis for D = 5 km is less significant due to the limited number of relic landslides. This result indicates that at least 10 relic landslides are required for a confident regression analysis. The appropriate D value for the analysis probably depends on the density of available relic landslides and the variety in environmental conditions (Fig. 4), although further studies are requied to discuss this issue.

(Table 3)

5. Conclusions

The present study explored the possibility of landslide maps for forecasting landslide travel distance. We analyzed the mobility of relic landslides outlined in the NIED landslide map in four landslide-prone areas, and examined the effects of size and initial slope on the H/L ratio of landslides. Inverse correlation between the H/L ratio and area of ruptured surface, A_r, was very weak, indicating a limited size effect under the scale of landslides shown in the NIED landslide map ($0.01 < A_r < 1$ km^2). Instead, the H/L ratio strongly correlates with the initial slope, i.e. slope of the ruptured surface, $\tan\theta_r$. On the $\tan\theta_r$–H/L charts, recent disaster-causing landslides were plotted near the 95% lower prediction limit of the regression lines for the relic landslides. Therefore, morphometric analysis of relic landslides in a given area enables us to predict the possible travel distance of an unstable mass in the area. In other words, detailed landslide maps may play an important role in forecasting landslide travel distance.

Acknowledgements

We thank Y. Matsukura for his comments on an early draft of the manuscript, and Nel Caine and one anonymous reviewer for their comments that improved the manuscript.

References

Ayalew, L., Yamagisghi, H., 2005. The application of GIS-based logistic regression for landslide susceptibility mapping in the Kakuda-Yahiko Mountains, Central Japan. Geomorphology 65, 15–31.

Carrara, A., Cardinali, M., Detti, R., Guzzetti, F., Pasqui, V., Reichenbach, P., 1991. GIS techniques and statistical models in evaluating landslide hazard. Earth Surface Processes and Landforms 16, 427–445.

Carrara, A., Crosta, G., Fratini, P., 2003. Geomorphological and historical data in assessing landslide hazard. Earth Surface Processes and Landforms 28, 1125–1142.

Chigira, M., Yagi, H., 2006. Geological and geomorphological characteristics of landslides triggered by the 2004 Mid Niigata prefecture earthquake in Japan. Engineering Geology 82, 202– 221.

Chigira, M., Chiba, T., Matsuura, S., 1998. Landslide-triggered steam explosion and debris flow at the Sumikawa Spa, Akita, Northern Japan, May 1997 (1) general view and geological background. Landslide News 11, 6–8.

Corominas, J., 1996. The angle of reach as a mobility index for small and large landslides. Canadian Geotechnical Journal 33, 260–271.

Cruden, D.M., Varnes, D.J., 1996. Landslide types and processes, In: Turner, A.K., Schuster, R.L. (Eds.), Landslides: Investigation and Mitigation (Transportation Research Council Special Report No. 247). National Academy Press, Washington D.C., pp. 36–75.

Finlay, P.J., Mostyn, G.R., Fell, R., 1999. Landslide risk assessment: prediction of travel distance. Canadian Geotechnical Journal 36, 556–562.

Guthrie, R.H., Evans, S.G., 2004. Analysis of landslide frequencies and characteristics in a natural system, coastal British Columbia. Earth Surface Processes and Landforms 29, 1321–1339.

Hayashi, S., Taniguchi, H., Chiba., T., 1998. Landslide-triggered steam explosion and debris flow at the Sumikawa Spa, Akita, Northern Japan, May 1997 (2) chronological records of events and steam explosions. Landslide News 11, 8–11.

Hoshino, M., Asai, K., 1997. The landslide disaster at Hachimantai-Sumikawa in May 1997 (preliminary report). Journal of the Geographical Survey Institute (Japan) 88, 28–40 (in Japanese).

Hsü, K.J., 1975. Catastrophic debris streams (Sturzstroms) generated by rockfalls. Geological Society of America Bulletin 86, 129–140.

Hunter, G., Fell, R. 2003. Travel distance angle for "rapid" landslides in constructed and natural soil slopes. Canadian Geotechnical Journal 40, 1123–1141.

IAEG Commission on Landslides, 1990. Suggested nomenclature for landslides. Bulletin of International Association of Engineering Geology 41, 13–16.

Innes, J.L., 1983. Lichenometric dating of debris-flow deposits in the Scottish Highlands. Earth Surface Processes and Landforms 8, 579–588.

Inokuchi, T., 1998. Landslide topography of the Sumikawa landslide. Journal of the Japan Landslide Society 35(2), 11–19 (in Japanese with English Abstr.).

Matsuura, S., Asano, S., Okamoto, T., Takeuchi, Y., Nakamura, S., 1998. Estimation of intensity of meltwater flowing out from the bottom of a snow pack prior to Hachimantai-Sumikawa landslide and its probability analysis using AMeDAS data set. Journal of the Japan Landslide Society 35(2), 20–28 (in Japanese with English Abstr.).

Moriwaki, H., 1987. A prediction of the travel distance of a debris. Journal of the Japan Landslide Society 24 (2), 10– 16 (In Japanese with English Abstr.).

Moriwaki, H., Hattanji, T., 2002. Morphometric analysis of landslides based on landslide maps. Journal of the Japan Landslide Society 39, 244–252 (in Japanese with English Abstr.).

Okunishi, K., 1982. Kinematics of large-scale landslides – A case study in Fukuchi, Hyogo Prefecture, Japan. Transactions, Japanese Geomorphological Union 3, 41–56.

Okunishi, K., Okuda, S., 1982. Refuge from large scale landslides – A case study: Nishiyoshino Landslide, Nara Prefecture, Japan. Journal Natural Disaster Science 4(2), 79–85.

Okura, Y., Kitahara, H., Kawanami, A., Kurokawa, U., 2003. Topography and volume effects on travel distance of surface failure. Engineering Geology 67, 243–254.

Ost, L., Van Den Eeckhaut, M., Poesen, J., Vanmaercke-Gottigny, M.C., 2003. Characteristics and spatial distribution of large landslides in the Flemish Ardennes (Belgium), Zeitschrift für Geomorphologie N.F. 47, 329–350.

Oyagi, N., Ikeda, H., 1998. Landslide structure and regional perspective on Sumikawa landslide at Hachimantai volcanic area, Northern Honshu, Japan. Journal of the Japan Landslide Society 35(2), 1–10 (in Japanese with English Abstr.).

Oyagi, N., Tanaka, K., Fukuzono, T., 1986. Report on the Jizukiyama landslide disaster on July 26, 1985 at Nagano city. Natural Disaster Research Report No. 26, NRCDP, Tsukuba, Japan, 45pp (in Japanese).

Oyagi, N., Terajima, H., Moriwaki, H., 1977. Report on the Fukuchi-Nukeyama Landslide disaster in Ichinomiya Town, Hyogo Prefecture and debris-flow disaster in Syodo Island, Kagawa Prefecture, due to Typhoon No. 17, 1977. Natural Disaster Research Report No. 13, National Research Center for Disaster Prevention (NRCDP), Tsukuba, Japan, 68pp (in Japanese).

Roering, J.J., Kirchner, J.W. Dietrich, W.E., 2005. Characterizing structural and lithologic controls on landsliding: Implications for topographic relief and landscape evolution in the Oregon Coast Range, USA. Geological Society of America Bulletin 117, 654–668.

Scheidegger, A.E., 1973. On the prediction of reach and velocity of catastrophic landslides. Rock Mechanics 5, 231–236.

Shimizu, F., Oyagi, N., 1985. Landslide Maps, Series 3 ”Hirosaki and Fukaura”. Technical Note No. 96, NRCDP, Tsukuba, Japan.

Shimizu, F., Oyagi, N., Inokuchi, T., 1984. Landslide Maps Series 2 ”Akita and Ojika”. Technical Note No. 85, NRCDP, Tsukuba, Japan.

Shimizu, F., Yagi, H., Higaki, D., Inokuchi, T., Oyagi, N. 2003. Landslide Maps, Series 16 “Nagano”. Technical Note No. 238, NIED, Tsukuba, Japan.

Shimizu, F., Oyagi, N., Miyagi, T., Inokuchi, T., 2004. Landslide Maps, Series 17 “Nagaoka and Takada”. Technical Note No. 244, NIED, Tsukuba, Japan.

Shimizu, F., Inokuchi, T., Oyagi, N., 2005a. Landslide Maps, Series 23 “Wakayama and Tanabe”. Technical Note No. 271, NIED, Tsukuba, Japan.

Shimizu, F., Inokuchi, T., Oyagi, N., 2005b. Landslide Maps, Series 24 “Himeji”. Technical Note No. 277, NIED, Tsukuba, Japan.

Yonetani, T., Moriwaki, H., Shimizu, F., 1983. Report on the debris-flow disasters in Isshi County, Mie Prefecture and Wada Landslide disaster in Nishiyoshino Village, Nara Prefecture, due to Typhoon No. 10, 1982. Natural Disaster Research Report No. 22, NRCDP, Tsukuba, Japan, 70pp (in Japanese).

Yoshimatsu, H., Abe, S., 2006. A review of landslide hazards in Japan and assessment of their susceptibility using an analytical hierarchic process (AHP) method. Landslides 3, 149–158.

Figure legends

Fig. 1. Section of landslide map 'Hachimantai' (Shimizu et al., 1984). Crowns are represented by thick solid lines, and displaced masses by thick broken lines.

Fig. 2. Locations of investigated areas.

Fig. 3. Topography and cross sections of recent landslides. (a) Sumikawa landslide (modified after Hoshino and Asai, 1997; Oyagi and Ikeda, 1998). (b) Jizukiyama landslide (Oyagi et al., 1986). (c) Wada landslide (Okunishi and Okuda, 1982; Yonetani et al., 1983). (d) Fukuchi landslide (Oyagi et al., 1977; and Okunishi, 1982). Hatched area shows residential area. Star in (a) shows the location of steam explosion. Different outlines for toe of displaced mass of Wada and Fukuchi landslides have been reported: (1) Okunishi and Okuda (1982), (2) Yonetani et al. (1983), (3) Okunishi (1982), and (4) Oyagi et al. (1977).

Fig. 4. Number of available relic landslides (a) and relative height (b) as a function of distance from recent landslides.

Fig. 5. Method for morphometric analysis of relic landslides.
(a) Definition of measured items. (b) Example of extrapolation for estimating foot elevation.

Fig. 6. Effect of landslide size on *H/L* ratio. Thin broken lines show regression lines for relic landslides.

Fig. 7. Effect of initial slope on *H/L* ratio. Broken lines show regression lines for

relic landslides. Thick solid lines show lower prediction limit with 95% probability for relic landslides.

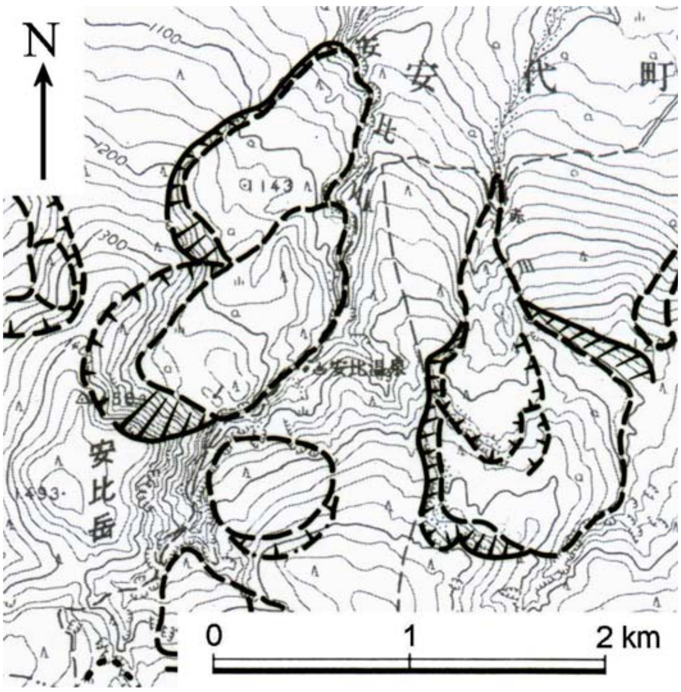

Fig. 1

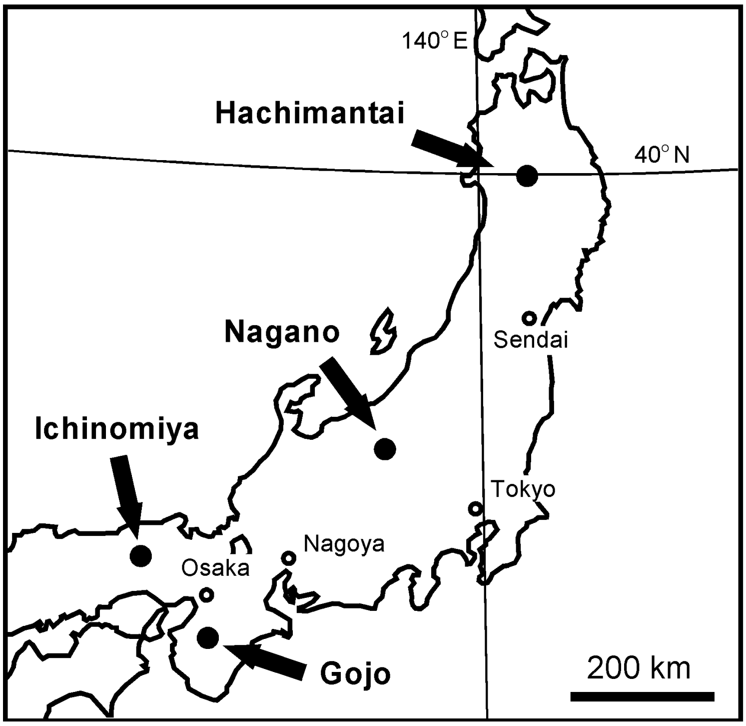
140° E
Hachimantai
40° N
Nagano
Sendai
Ichinomiya
Tokyo
Nagoya
Osaka
Gojo
200 km

Fig. 2

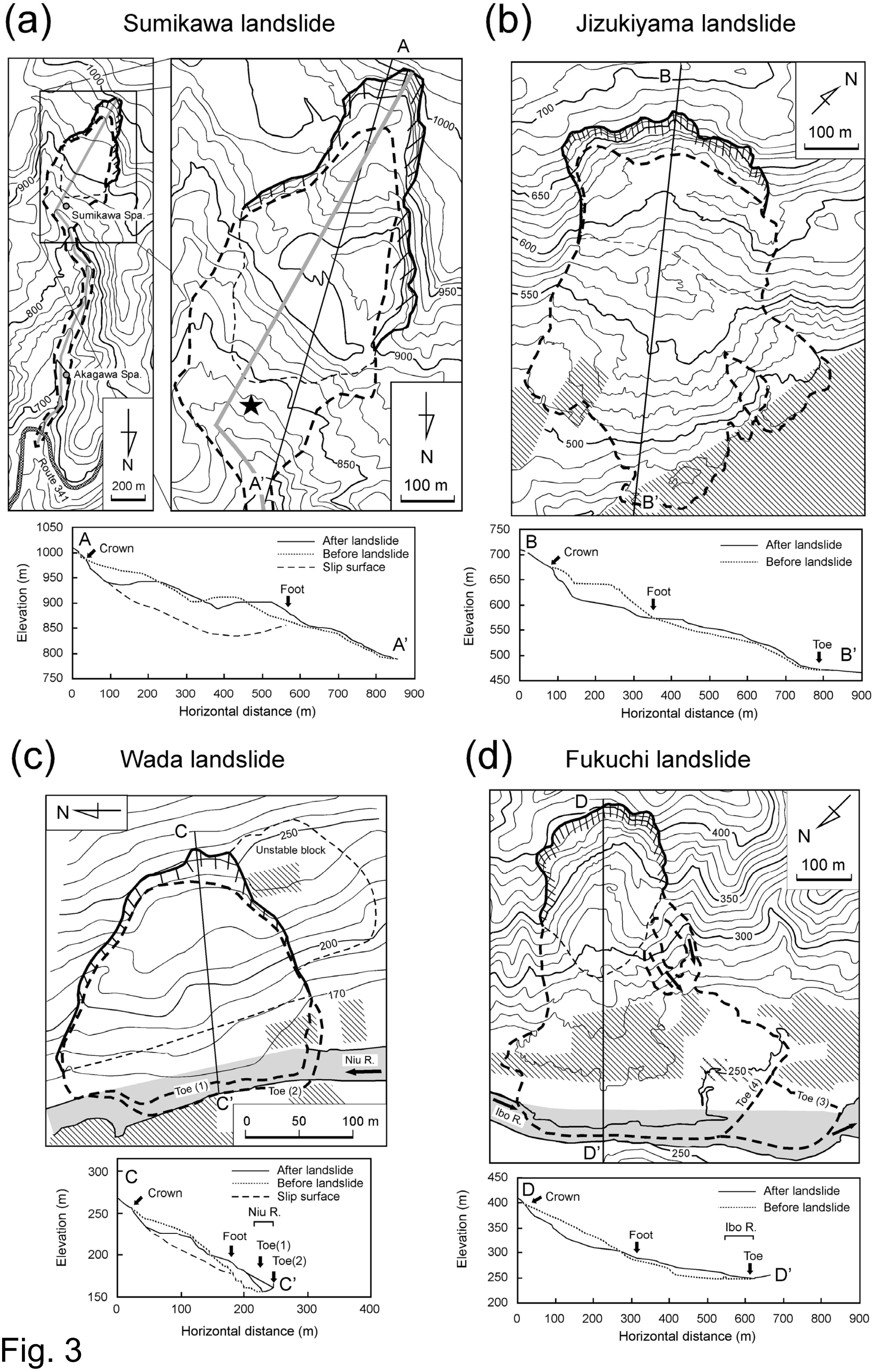

(a)
Sumikawa landslide
A
1000
900
Sumikawa Spa.
800
Akagawa Spa.
700
Route 341
N
200 m
950
900
850
A'
N
100 m
Crown
After landslide
Before landslide
Slip surface
Foot
Elevation (m)
Horizontal distance (m)
(b)
Jizukiyama landslide
B
N
100 m
700
650
600
550
500
B'
Crown
Foot
Toe
After landslide
Before landslide
Elevation (m)
Horizontal distance (m)
(c)
Wada landslide
N
C
250
Unstable block
200
170
Niu R.
Toe (1)
Toe (2)
C'
0
50
100 m
Crown
After landslide
Before landslide
Slip surface
Niu R.
Foot
Toe(1)
Toe(2)
Elevation (m)
Horizontal distance (m)
(d)
Fukuchi landslide
D
400
N
100 m
350
300
250
Toe (4)
Toe (3)
Ibo R.
D'
250
Crown
After landslide
Before landslide
Foot
Ibo R.
Toe
Elevation (m)
Horizontal distance (m)

Fig. 3

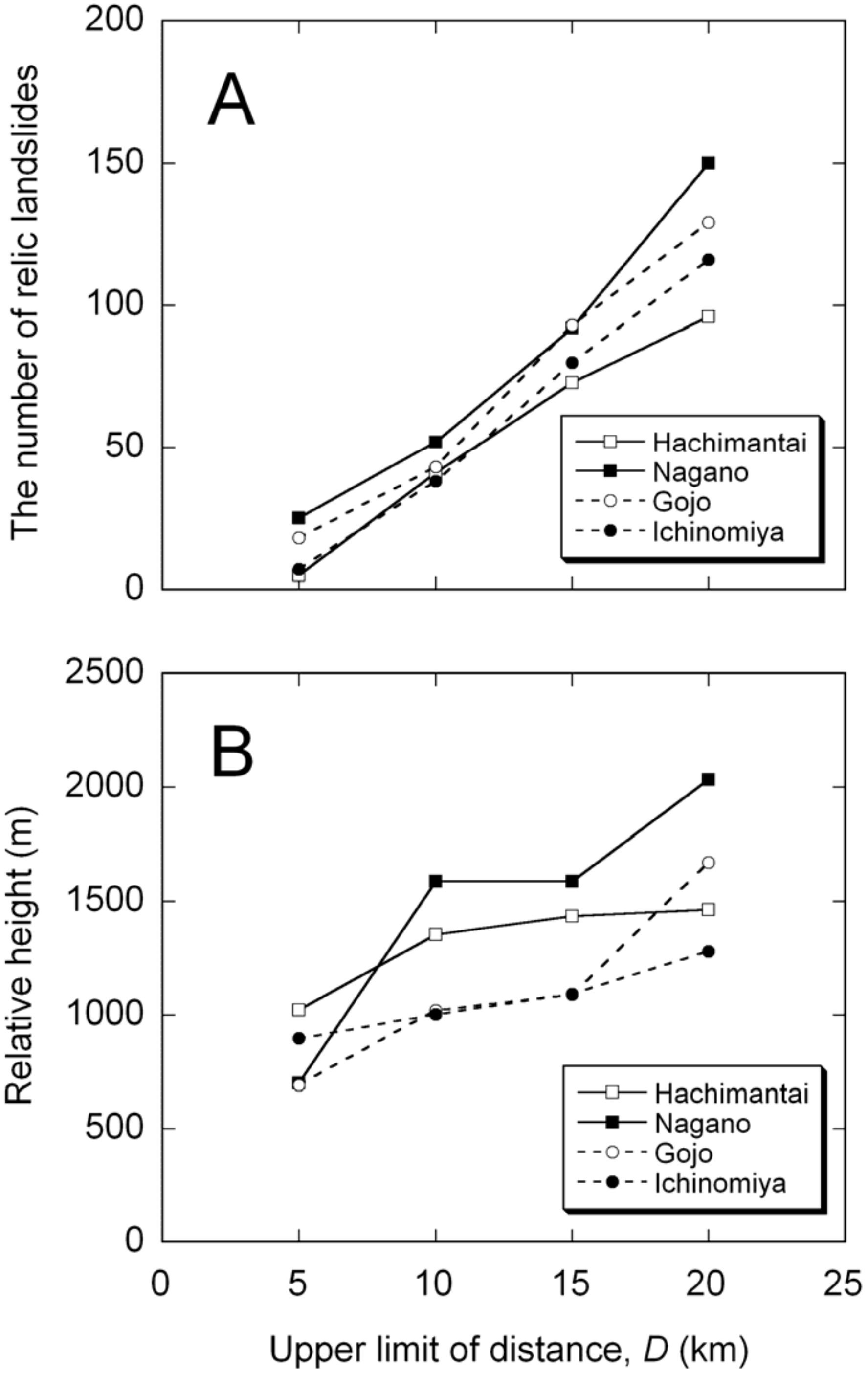
A
B
The number of relic landslides
Relative height (m)
Upper limit of distance, D (km)
Hachimantai
Nagano
Gojo
Ichinomiya
0
50
100
150
200
500
1000
1500
2000
2500
5
10
15
20
25

Fig. 4

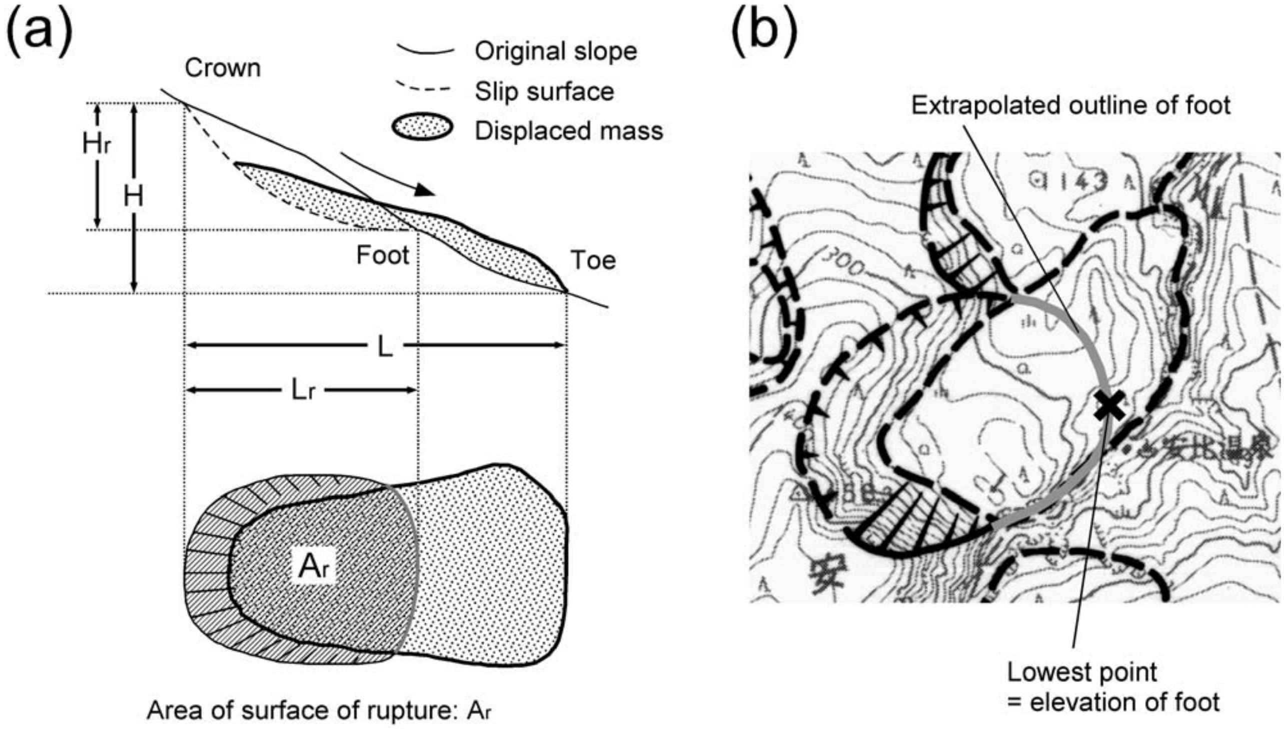
(a)
Crown
Original slope
Slip surface
Displaced mass
Hr
H
Foot
Toe
L
Lr
Ar
Area of surface of rupture: Ar
(b)
Extrapolated outline of foot
Lowest point
= elevation of foot

Fig. 5

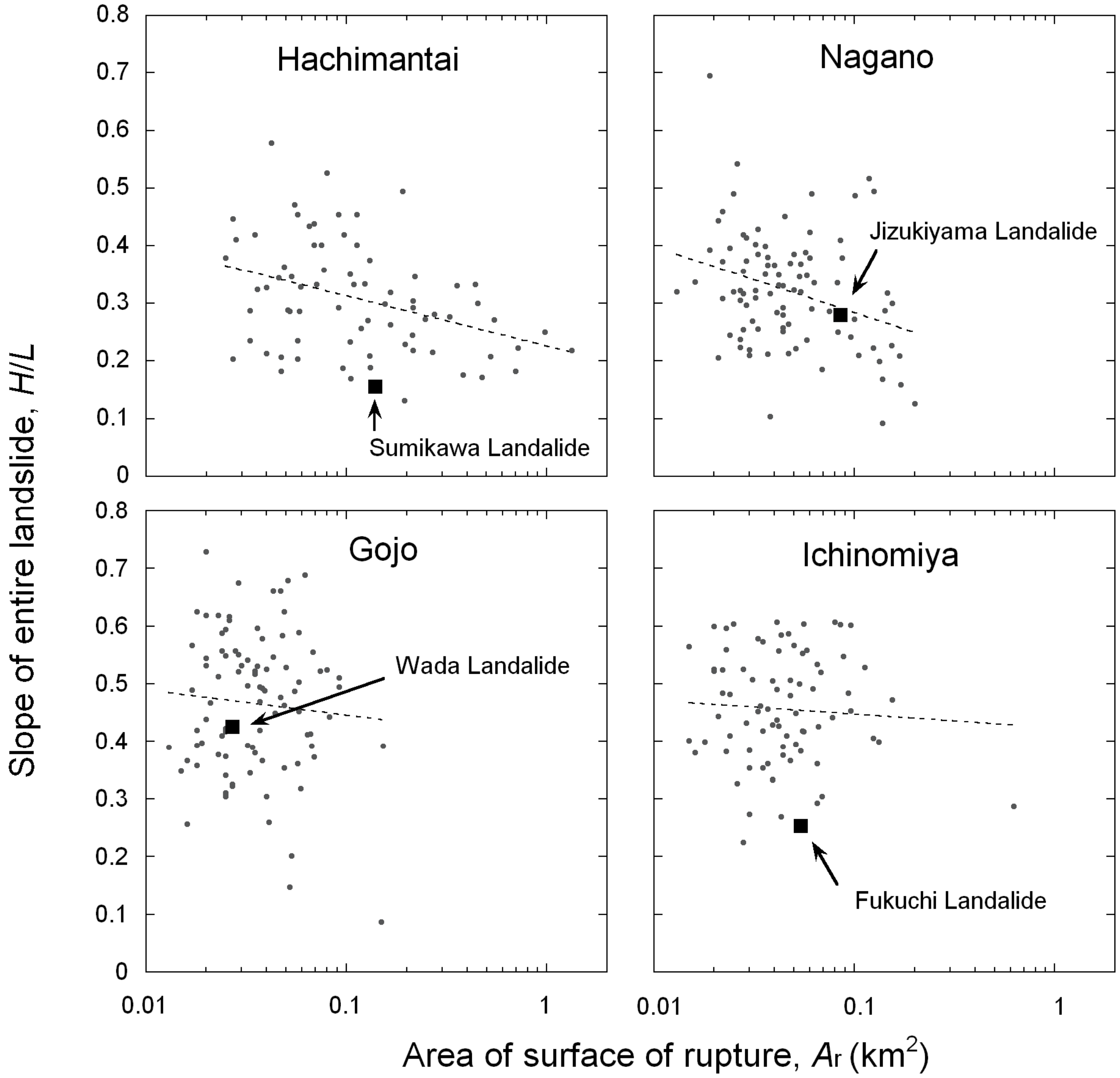

Hachimantai
Sumikawa Landalide
Nagano
Jizukiyama Landalide
Gojo
Wada Landalide
Ichinomiya
Fukuchi Landalide
Slope of entire landslide, H/L
Area of surface of rupture, Ar (km2)
0
0.1
0.2
0.3
0.4
0.5
0.6
0.7
0.8
0.01
0.1
1

Fig. 6

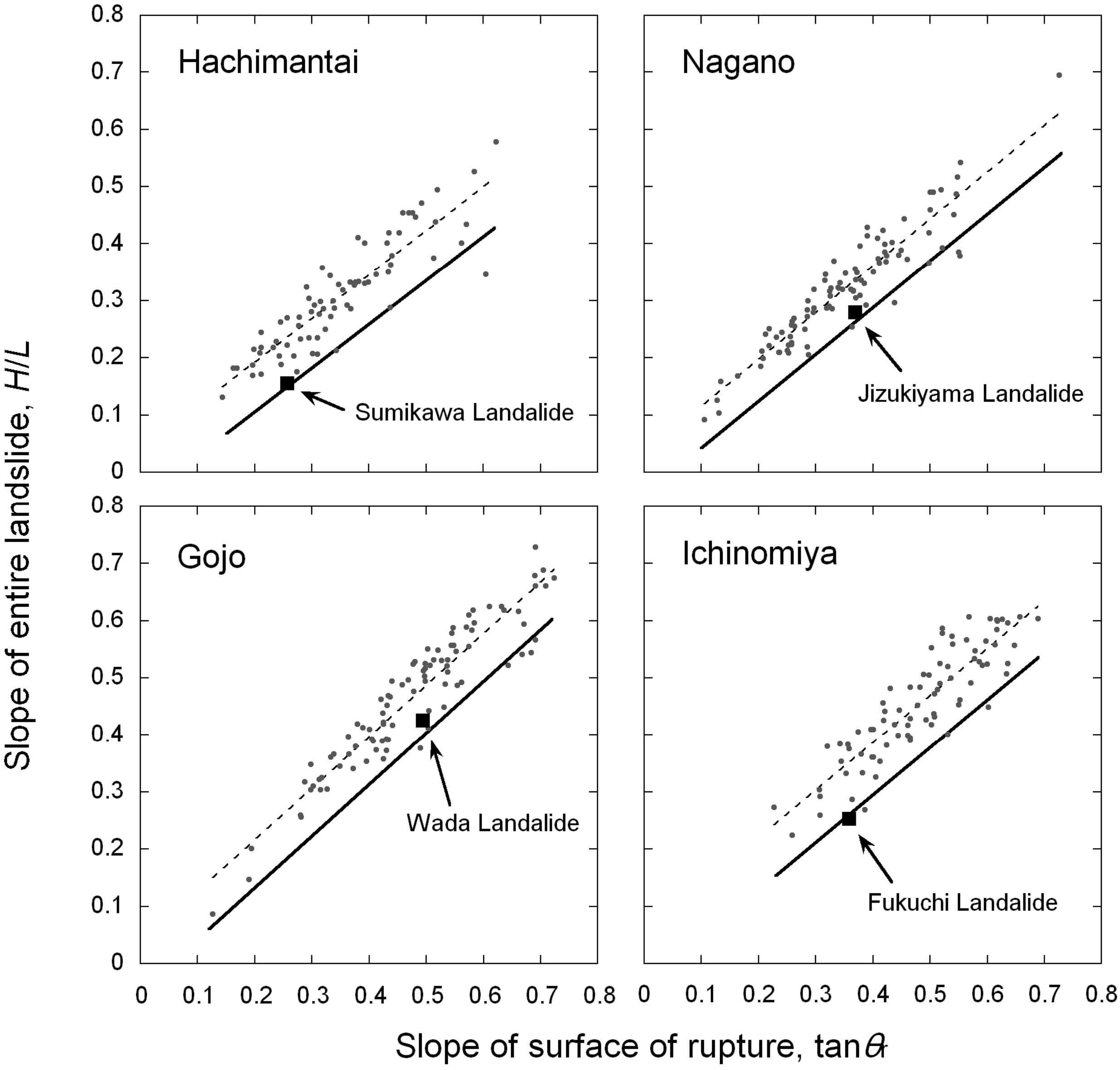

Hachimantai
Nagano
Gojo
Ichinomiya
Sumikawa Landalide
Jizukiyama Landalide
Wada Landalide
Fukuchi Landalide
Slope of entire landslide, H/L
Slope of surface of rupture, tanθ
0
0.1
0.2
0.3
0.4
0.5
0.6
0.7
0.8

Fig. 7

Tables

Table 1. Environmental conditions of investigated areas.

Investigated area	Main geology*	Precipitation** (mm/yr)	Temperature** (°C)	Altitude range (m)	Landslide area (%)
Hachimantai	VR (Q,N) with SR (N)	1880	6.9	1613 – 180	23.1
Nagano	SR (N) with VR(Q,N)	900	11.7	1917 – 330	13.0
Gojo	SR (M) with crystalline schist	1370	14.5	1177 – 82	5.3
Ichinomiya	VR (M), SR (M) with granodiorite	1770	13.3	1730 – 61	3.7

*VR: volcanic rocks, SR: sedimentary rocks, (Q): Quaternary, (N): Neogene, (M): Mesozoic.

**annual mean for recent 22–30 years observed at Japan Meteorological Agency automated meteorological stations (AMeDAS). The name of the referred station is same as the name of each investigated area.

Table 2. Geometry of recent landslides. Area of rupture surface, A_r; relative height of entire landslide, H; length of entire landslide, L; slope of rupture surface, $\tan\theta_r$.

Name of landslide	Investigated area	A_r (km^2)	H (m)	L (m)	H/L	$\tan\theta_r$
Sumikawa	Hachimantai	0.139	350	2250	0.156	0.256
Jizukiyama	Nagano	0.085	205	732	0.280	0.369
Wada	Gojo	0.027	95	223	0.426*	0.494
Fukuchi	Ichinomiya	0.054	152	600	0.253	0.358

*calculated from outline (2)

Table 3. The 95% lower prediction limits calculated from initial slope of recent landslides and datasets of relic landslides for different *D* values.

	Hachimantai	Nagano	Gojo	Ichinomiya
H/L, recent	0.156 (Sumikawa)	0.280 (Jizukiyama)	0.426 (Wada)	0.253 (Fukuchi)
D = 5 km	n.s. (N =5)*	0.269 (N = 25)	0.383 (N = 18)	0.229 (N = 7)**
D = 10 km	0.132 (N = 40)	0.261 (N =52)	0.384 (N = 43)	0.259 (N =38)
D = 15 km	0.149 (N = 73)	0.263 (N = 92)	0.399 (N = 93)	0.260 (N = 80)

* analysis not significant (p > 0.05), ** analysis less significant (p ~ 0.01)